

Scaling Theory and Numerical Simulations of Aerogel Sintering

Rémi Jullien, Nathalie Olivi-Tran, Anwar Hasmy, Thierry Woignier, Jean Phalippou,
Daniel Bourret and Robert Sempéré

*Laboratoire de Science des Matériaux Vitreux, Université Montpellier II, Place Eugène Bataillon,
34095 Montpellier, France*

(March 26, 2021)

Abstract

A simple scaling theory for the sintering of fractal aerogels is presented. The densification at small scales is described by an increase of the lower cut-off length a accompanied by a decrease of the upper cut-off length ξ , in order to conserve the total mass of the system. Scaling laws are derived which predict how a , ξ and the specific pore surface area Σ should depend on the density ρ . Following the general ideas of the theory, numerical simulations of sintering are proposed starting from computer simulations of aerogel structure based on a diffusion-limited cluster-cluster aggregation gelling process. The numerical results for a , ξ and Σ as a function of ρ are discussed according to the initial aerogel density. The scaling theory is only fully recovered in the limit of very low density where the original values of a and ξ are well separated. These numerical results are compared with experiments on partially densified aerogels.

PACS numbers: 61.43.Hv, 64.60.Ak, 81.20.Ev.

Typeset using REVTeX

I. INTRODUCTION

Sintering of silica aerogels is a process in which the original material is heated at a temperature smaller than the melting temperature of the corresponding silica crystal. It results in a strengthening of the internal structure and a gradual elimination of the pores accompanied by a general densification and shrinkage of the whole sample. Such process allows the design of intermediate materials, hereafter called PDA (partially densified aerogels) of increasing density up to full dense silica glass. Several theories have been introduced to explain the shrinkage due to sintering [1–5]. It is now quite well established that the internal mechanism for sintering of aerogels is due to local viscous flows of matter. For the application to glasses and aerogels, the most convincing theoretical approaches are due to Scherer [4,5]. Here, we present a scaling approach, which can be considered as a generalization of Scherer’s type of calculations to fractal matter. Since a short account of the theory has already been published elsewhere [6], we present here a slightly different (simpler) derivation of the scaling laws (part 2A). Based on these theoretical ideas, we present two recently developed numerical procedures able to simulate the sintering of realistic aerogel structures (part 2B). Then, after presenting the numerical results (part 3), we compare them with experiments (part 4) and we conclude (part 5).

II. CONSTRAINTS ON THEORY

A. Scaling theory

It is now well established (see for example the recent interpretation of low angle neutron scattering experiments [7]) that silica aerogels are made of connected fractal aggregates. Fractal scaling occurs in a range of lengths extending from a lower cut-off a , which is the mean diameter of the silica particles constituting the aggregates, up to an upper cut-off ξ which is the mean diameter of the aggregates, or, equivalently, the mean center-to-center distance between two neighboring connected aggregates. Since it is admitted that,

in aerogels, sintering results from local viscous flow of matter, we will assume that only the shortest lengths are concerned and therefore only the lower cut-off a is affected, without changing neither the fractal dimension of the aggregates nor their mutual arrangement. After a first stage where the individual shapes of silica particles are only slightly modified, while bridges are built between them, one reaches a “scaling” regime where individual particles can no longer be distinguished. In this regime, we will assume that there still exist a lower cut-off a , which can then be defined as the mean thickness of the aggregates arms. Since the sintering process tends to lower the internal surface pore area by transferring matter from large curvature to small curvature regions and therefore reinforcing the thinner arms, there results a gradual increase of a . But, correlatively, to insure the mass conservation, there should be a general shrinkage of the material, characterized by a decrease of ξ . Figure 1 gives a two-dimensional sketch of how an aggregate looks like at two different stages of sintering.

Since we assume that the overall inter-aggregate structure is conserved, the shrinkage at the scale of an aggregate is the same as at the macroscopic scale. Therefore, if ρ is the mean density of the material, the following “trivial” scaling should hold:

$$\xi \sim \rho^{-\frac{1}{3}} \quad (1)$$

Then, using the results of the fractal geometry for simple scale-invariant structures [8], the minimum number N of balls of diameter a necessary to cover the total mass of a fractal aggregate of diameter ξ (the requirement being that each point of silica matter should be inside at least one ball), is given by:

$$N \sim \left(\frac{\xi}{a}\right)^D \quad (2)$$

Very often, this formula appears in the literature with only one parameter (a or ξ) because the other one is assumed to stay constant. Given a , the relation $N \sim \xi^D$ corresponds to the “mass-size” relation. Given ξ , the relation $N \sim a^{-D}$ corresponds to the Hausdorff-Besicovitch definition of the fractal dimension (for simple self-similar fractals all the definitions of the fractal dimension lead to the same value [8]). But here, we need to keep the

two parameters together since they both vary. Using this formula, the bulk density can be expressed as a function of a and ξ :

$$\rho \sim \frac{Na^3}{\xi^3} \sim \left(\frac{a}{\xi}\right)^{3-D} \quad (3)$$

Then, combining with equation (1), we immediately get:

$$a \sim \rho^{D/3(3-D)} \quad (4)$$

Even if the present derivation of equation (4) is more straightforward than the one already given [6], it implicitly uses the same simple symetries (fractal scaling and mass conservation).

As soon as a and ξ are known, any other structural property, which is related to these parameters, can be calculated. Several examples have been previously provided [6] but here we will focus on the specific pore surface area Σ which is the area of the whole silica-air interface counted per unit of silica mass. Following the above ball-covering reasoning, the total interface for one aggregate, is of order Na^2 while its mass is of order Na^3 , therefore one has:

$$\Sigma \sim \frac{Na^2}{Na^3} \sim \frac{1}{a} \sim \rho^{-D/3(3-D)} \quad (5)$$

A key point of our reasoning is that a remains a well defined cut-off. In other words the constitutive aggregates can be modeled by *mass fractals* downs to length a . Therefore to satisfy (1) and (3) simultaneously, a should increase if ξ decreases and reciprocally. Such reasoning fails if the interface might be considered as a *surface fractal*; then one could imagine to smooth the surface without changing ξ . This may happen for other kind of materials and, here, for the last stages of sintering where the scaling theory doesnot work.

Before pursuing, it might interesting to compare our scaling results with previous Scherer's approach of sintering [4,5]. In its first calculation [4], Scherer was considering a regular cubic array whose bonds were made of cylinders of length ξ and diameter a . Neglecting surface deformations near the cylinders connections and simulating the sintering as

an increase of a/ξ , he was able to calculate analytically the density as a function of a/ξ , at least for $a < \xi$:

$$\frac{\rho}{\rho_S} = 3\pi\left(\frac{a}{\xi}\right)^2 - 8\sqrt{2}\left(\frac{a}{\xi}\right)^3 \quad (6)$$

where ρ_S is the density of silica. This formula can be usefully compared with our formula (3). Since Scherer is considering the peculiar case of $D = 1$ fractals his first term is the same as ours, but, in his simple geometry, he is able to perform the full analytical calculation and he gets a second term which, in our language, appears to be a correction to scaling since it is negligible compared to the first term when ξ/a is large.

B. Numerical simulations

Since it has been shown that the diffusion-limited cluster-cluster aggregation model [9,10] provides a quite realistic modelization of an aerogel structure [7,11], in this section we intend to use such a model to develop numerical simulations of aerogel sintering. This is still an approximate treatment of sintering since we will use some naive coarse-graining procedures, such as that used in real-space renormalization group methods [12], to describe the smoothing at the shortest scale, but, since we are now considering a realistic structure, we hope to get some informations on corrections to scaling.

We have developed two numerical methods. The first one works on a cubic lattice and considers cubic particles of edge length a_0 (volume $v_0 = a_0^3$, mass $m_0 = \rho_S a_0^3$). The second one works off-lattice and considers spherical particles of diameter a_0 (volume $v_0 = \frac{\pi}{6} a_0^3$, mass $m_0 = \frac{\pi}{6} \rho_S a_0^3$). In both cases the particles are inside a cubic box of edge length La_0 and their number N_0 is such that the volume fraction c_0 is set to a desired value $c_0 = N_0 v_0 / L^3 a_0^3$. Therefore, except L which should be chosen as large as possible, the only parameter of the model is c_0 which is directly related to the initial aerogel density $\rho_0 = c_0 \rho_S$.

To build the original (non-sintered) aerogel structure, the particles are first randomly disposed (i. e. put on randomly chosen sites, avoiding multiple occupancy, on lattice, or

sequentially centered at random points, avoiding overlaps, off-lattice) in the box. Then, these particles are allowed to undergo a brownian diffusive motion and they irreversibly stick when come on contact. Aggregates of particles are also able to diffuse together with the individual particles and to stick to particles or to other aggregates. In this diffusive motion, the diffusion constant of the aggregates is considered to vary as the inverse of their radius of gyration and periodic boundary conditions are assumed at the box edges [9–11]. When the concentration c_0 is sufficiently large (larger than a threshold value c_g which tends to zero for infinite box size [7]), the final structure is a gelling network which extends from edge to edge in the box and which can be described as a loose random packing of connected fractal aggregates, of fractal dimension $D \simeq 1.8$, whose mean size ξ_0 decreases as c_0 increases.

The modelization of the sintering process differs if one considers the on-lattice or the off-lattice version of the model.

1. On lattice

Here we have used a discrete blocking method (based on “box counting” ideas [8]) which proceeds step by step. It implies that the value of L is set to some power of 2, $L = 2^n$. At step p of sintering, the original cubic lattice is replaced by a “super-lattice” of parameter length $2^p a_0$, each super-cell of the new lattice containing 2^{3p} cells of the original lattice. Then a super-cell is considered as occupied if it contains at least one particle of the original structure. The number N_p of occupied super-cells is computed. Then the sintered structure is obtained by considering the structure made of the N_p occupied super-cells and by applying an adequate length contraction β_p in order to conserve the total mass. The volumic fraction c_p of the super-structure being:

$$c_p = \frac{N_p (2^p a_0)^3}{(L a_0)^3} = 2^{3p} \frac{N_p}{N_0} c_0 \quad (7)$$

the contraction factor is given by:

$$\beta_p = \left(\frac{c_p}{c_0}\right)^{\frac{1}{3}} = 2^p \left(\frac{N_p}{N_0}\right)^{\frac{1}{3}} \quad (8)$$

and the actual value of the cut-offs a_p and ξ_p at step p are given by:

$$a_p = 2^p \frac{a_0}{\beta_p} = \left(\frac{N_p}{N_0}\right)^{\frac{1}{3}} a_0 \quad (9)$$

$$\xi_p = \frac{\xi_0}{\beta_p} \quad (10)$$

As expected when combining formulae (8) and (10) one recovers that the “trivial” scaling law (1) on ξ is automatically satisfied, but the one on a deserves to be tested by the numerical calculations. On figure 2 (a) we provide a typical example where a section of the box is shown at three different steps of sintering.

To determine the specific pore surface area, we numerically determine the number S_p of square interfaces separating occupied supercells nearest neighbor to a non-occupied one (taking care of the periodic boundary conditions) and we calculate Σ by:

$$\Sigma_p = \frac{1}{\rho_S} \frac{S_p a_p^2}{N_p a_p^3} = \frac{1}{a_0 \rho_S} \frac{S_p}{N_p^{\frac{2}{3}} N_0^{\frac{1}{3}}} \quad (11)$$

In practice, for a given c_0 and at each step p , the quantities N_p and S_p , calculated numerically, have been averaged over several realizations of the initial configuration.

Note that we could have removed the restriction to supercells of edge lengths $2^p a_0$, working instead with edge lengths ℓa_0 , ℓ being any integer. Imagining such an extension of the method, let us call ℓ_f the value of ℓ above which all the supercells become occupied and define ξ_0 as being $\ell_f a_0$. With this definition ξ_0 is not, rigourously speaking, the mean aggregate diameter but, rather, it is such that $\xi_0 - a_0$ represents the edge length of the largest cubic hole in the structure. Using then the fact that, at the end of the sintering process, one has $\xi_f = a_f$, one gets:

$$a_f = \xi_0 c_0^{-\frac{1}{3}} \quad (12)$$

In practice we have written a separate code to evaluate ξ_0 by determining ℓ_f . Therefore using (12), one can get a numerical estimate of a_f .

2. Off lattice

Here we have used a dressing method which, compared to the preceding method, has the advantage to be continuous. We first consider a s -dependent dressed structure, where s is a continuous variable, in which each initial sphere of diameter a_0 is replaced by a sphere of the same center but of larger diameter $a_d(s)$, given by:

$$a_d(s) = a_0(1 + s) \quad (13)$$

Then the total volume $V_d(s)$ located inside the overlapping spheres is numerically calculated (avoiding multiple counting of overlaps). The volumic fraction of the dressed structure is given by:

$$c(s) = \frac{V_d(s)}{(La_0)^3} \quad (14)$$

Here also, to insure mass conservation, the sintered structure is obtained from the dressed structure after applying an adequate length contraction $\beta(s)$ given by:

$$\beta(s) = \left(\frac{c(s)}{c_0}\right)^{\frac{1}{3}} = \left(\frac{6V_d(s)}{N\pi a_0^3}\right)^{\frac{1}{3}} \quad (15)$$

Then the actual diameter $a(s)$ of the spheres of the sintered structure and the correlation length $\xi(s)$ are given by:

$$a(s) = \frac{a_d(s)}{\beta(s)} = a_0 \frac{1 + s}{\beta(s)} \quad (16)$$

$$\xi(s) = \frac{\xi_0}{\beta(s)} \quad (17)$$

Here again the scaling law on $\xi(s)$ is automatically verified while $a(s)$ needs a numerical calculation. The value for ξ_0 is estimated from a_f , the limiting value of $a(s)$ when $c(s)$ tends to one, by inverting formula (12). Here $\xi_0 - a_0$ represents the diameter of the largest spherical hole. On figure 2(b) we provide a typical example where a section of the box is shown at three different steps of sintering.

To determine the specific pore surface area $\Sigma(s)$, we observe that the total surface $S_d(s)$ of the dressed structure is simply related to the derivative of the function $V_d(s)$:

$$S_d(s) = 2 \frac{dV_d}{da_d} = \frac{2}{a_0} \frac{dV_d(s)}{ds} \quad (18)$$

Then, dividing by the total mass and correcting by the adequate scaling factor, we get the following expression $\Sigma(s)$:

$$\Sigma(s) = \frac{2}{a_0 \rho_S} \frac{1}{V_d(s)} \frac{dV_d}{ds} \beta(s) = \frac{2}{a_0 \rho_S} \frac{d \log c(s)}{ds} \beta(s) \quad (19)$$

In practice, for a given c_0 , we have numerically determined the whole curve $c(s)$ versus s as well as its derivative and we have calculated, $a(s)$ and $\Sigma(s)$ using formulae (16) and (19). Here also, for each c_0 value, the results have been averaged over several realizations of the initial configuration.

III. RESULTS

In both the on-lattice and off-lattice cases, we have made calculations with $L = 64$, we have considered initial concentrations $c_0 = 0.01, 0.02, 0.05$ and 0.1 and the results for c , a and Σ have been averaged over 20 independent realizations of the initial configuration. Figure 3 gives the results for a/a_0 and ξ/a_0 as a function of c (log-log plot) for the different c_0 values. Cases (a) and (b) correspond to on-lattice (symbols) and off-lattice (continuous lines) results, respectively. The slope indicated is the theoretical slope $D/3(3 - D) = 0.5$ expected from the scaling theory with $D = 1.8$. In principle, the scaling theory should be recovered in the vanishing concentration limit $c_0 \rightarrow 0$ where a_0 and ξ_0 are well separated. Even if the results for a versus c are more and more linear, with an apparent slope close to 0.5, when c_0 decreases, in both cases we observe, down to $c_0 = 0.02$, some corrections to scaling both at low c and large c .

The low- c corrections to scaling are different in the two simulations. When performing a low- s expansion in the off-lattice formulae, it can be shown that a in this case should behave quadratically when c tends to c_0 :

$$\left(\frac{a - a_0}{a_0}\right)_{\text{off}} \sim \left(\frac{c - c_0}{c_0}\right)^2 \quad (20)$$

This singular behavior is due to the peculiar non sintered structure made of perfectly tangent spheres. In all other situations, with non zero areas between connected particles, as it is in the on-lattice case, the low- c behavior should be linear:

$$\left(\frac{a - a_0}{a_0}\right)_{\text{on}} \sim \frac{c - c_0}{c_0} \quad (21)$$

Therefore, in the off-lattice case, there is an initial regime during which finite areas are grown between connected particles. During this regime, for the same increase of ρ , a increases less than in the on-lattice case. After this regime, the evolution of a becomes similar to the one of the on-lattice case, but for a larger initial concentration. This is shown in figure 4 (a) where we have reported the off-lattice results for $c_0 = 0.01$ (dashed curve), which, except at low concentrations, are very close to the on-lattice results for $c_0 = 0.02$. Note that, apart from low- c corrections to scaling, the lattice structure built with spherical particles of diameter a_0 , instead of cubes, which has a concentration smaller ($c'_0 = (\pi/6)c_0$), behaves quite similarly during sintering. This is reasonable, since, starting from the same spheres it is known that the on-lattice and off-lattice diffusion limited cluster-cluster aggregation processes lead to the same large distance correlations [13].

At large c (c close to 1) the correction to scaling comes from the fact that, in this limit, it remains only a few holes in the structure and, obviously, one can no longer speak of a structure made of connected fractals. The volume fraction of the last hole being $1 - c$ and its radius being proportional to $a_f - a$, where a_f is the limiting value of a , one should have:

$$a_f - a \sim (1 - c)^{\frac{1}{3}} \quad (22)$$

This behavior is well verified by both on-lattice and off-lattice numerical results.

Concerning the specific pore surface area, we have calculated the dimension-less quantity $a_0\rho_0\Sigma$. It is worth noticing that we get different results already for $c = c_0$. In the off-lattice case, we recover the trivial result:

$$(a_0\rho_0\Sigma_0)_{\text{off}} = 6 \tag{23}$$

which means that the structure is made of non-overlapping spheres. In the on-lattice case, we get a lower value since we do not count the interfaces between neighboring particles. If we neglect the contributions of loops, it can be shown that the 6 should be replaced by $4 - 2/N_0$ (since there should be $N_0 - 1$ bonds). But, due to the presence of loops, the actual number is smaller, close to 3.5 and decreases when c_0 increases. The numerical results for Σ as a function of c are given in figures 4 (a) and (b) as a log-log plot of $\frac{\Sigma}{\Sigma_0}$ versus c for the different c_0 values. In both cases the slope -0.5 expected from the scaling theory is better verified than for a . Here also the c_0 for the off-lattice case is close to the curve for $c'_0 = c_0/2$ for the on-lattice case (but not as close as in the case of a). When c tends to 1, we recover that Σ tends to zero, which is an improvement compared to the toy model. Following the above reasoning for c close to 1, one should get:

$$\Sigma \sim \frac{1}{a_f - a} \sim (1 - c)^{-\frac{1}{3}} \tag{24}$$

a behavior quite well observed in our off-lattice results.

Another result of our numerical calculations is the estimate of ξ_0 , which is here related to the largest spherical hole in the non sintered aerogel. In table I, we compare our off-lattice results with the alternative estimates (here called ξ'_0) obtained from the location of the minimum of the pair correlation function $g(r)$ [7]. It is reasonable that these estimates are close and roughly proportional to each other.

IV. DISCUSSION

In this section we would like to discuss our numerical results at the light of several experimental results on partially densified aerogels (PDA). Let us discuss first some previous low angle neutron diffraction experiments [14]. In figure 6, we show the scattering intensity $I(q)$ curves for a series of PDA of increasing densities made by sintering a “neutral” aerogel, hereafter called N46. These experimental results are in good qualitative agreement with the

theory. The slope of the fractal linear regime (here corresponding to $D \sim 2.3$) does not depend on the density, except in the last steps of sintering (where anyway the slope can no more be interpreted as a fractal dimension), but its q extension is gradually reduced as ρ increases. The arrows show how the parameter a and ξ have been previously estimated, i. e. by assuming that a^{-1} and ξ^{-1} correspond to the lower and upper departures from linearity. At the light of the recent interpretation of the $I(q)$ curves for non-sintered aerogels [7], we now know that such method is approximate and cannot give the right absolute values for both a and ξ . In particular, since ξ should be related to the position of the low- q maximum, not visible on the figure, its actual value should be considerably larger than the above estimate. However, since the estimation has been done with exactly the same procedure for all densities, we can think that the relative values a/a_0 and ξ/ξ_0 are relevant. The same method has been applied for another neutral sample, N26, of lower initial density but of similar fractal dimension and on a basic sample, B46 of lower fractal dimension $D \sim 1.8$, for which it is believed that the DLCA model applies [7].

Figure 6 (a) gives the results obtained with the basic sample as a log-log plot of both a/a_0 and ξ/a_0 versus ρ/ρ_S and the best fits of a/a_0 with both calculations. The continuous curve is the result of the off-lattice calculation with $c_0 = 0.04$ and the circles correspond to the on-lattice calculation with $c_0 = 0.08$. Since the actual density of the non-sintered sample is about 0.2g/cm^3 , the experimental c_0 value should be about 0.09, closer to the value taken for the on-lattice fit. The fact that the on-lattice model works better is certainly due to the presence of finite areas between connected particles already in the non-sintered material. Such “pre-sintering” might have occurred during the supercooling process used to obtain the aerogel from the gel by extracting the solvent. The data for a are quite well fitted except for the point of largest density. Anyway, since this point corresponds to a very large density, the method of determining a from the $I(q)$ data becomes highly questionable. Note that in the last stages of sintering, one cannot interpret $I(q)$ by the fractal theory and one needs another numerical calculations of $I(q)$ (such as the scattering by a collection of random polydisperse holes of radii $a_f - a$ at averaged mutual distance ξ) to be able to interpret the

scattering curves. Moreover the numerical estimates of ξ (except the last point) exhibit a nice $-1/3$ slope providing a strong support to the main hypothesis of our theory. However the estimates are smaller (by a factor almost 5) than the theoretical values, as expected if one remembers that the theoretical ξ_0 value is related to the location of the maximum of the $I(q)$ curve.

Figure 6 (b) gives the experimental results for two neutral samples with different initial densities. Here we cannot try to quantitatively compare with our numerical results since the fractal dimension is larger. It is known that the formation of neutral aerogels cannot be explained by the DLCA model. They have a tenuous and flexible polymeric structure and therefore deformations and restructuring cannot be avoided during aggregation. However the effective slope of the a versus c curves is larger than in the basic case in perfect agreement with the scaling theory, as already mentioned in [6]. Assuming a fractal dimension of 2.3, the theoretical slope $D/3(3 - D)$ should be slightly larger than 1. Assuming that the corrections to scaling enters similarly than in the basic case, the experimental slope is smaller as seen in the figure. Moreover, here again, the results for ξ exhibit a nice $-1/3$ slope.

V. CONCLUSION

In this contribution we have presented a scaling model for the sintering of aerogels, we have etayed this approach by some numerical calculations and we have compared the numerical results with some experiments. The numerical calculations have shown that corrections to scaling are not negligible, in particular at the last stages of sintering where the fractal scaling process is no more valid (the notion of cut-off fails) and where the sintering process rather involves a gradual elimination of residual holes. In the first stages of sintering the corrections to scaling have a larger role in the c -dependence of the lower cut-off a than in that of the specific pore surface area. The effective slope of the numerical $\log a$ versus $\log c$ curve is slightly smaller than the one expected from the scaling theory. These theoretical results are in quantitatively and qualitatively good agreement with experimental results on

basic and neutral aerogel, respectively. A quantitative agreement in the case of neutral aerogels requires a specific modelization of these materials which have a larger fractal dimension than basic aerogels. Nevertheless, the numerical calculations presented here are still using crude modelizations of what might be the actual sintering process. Even if the two numerical methods presented here give almost the same results, in both cases, at each step of sintering, the internal surface of the pores is not a minimum area surface as it should be. In particular, in the last stages of sintering, the remaining holes are not spherical. A more sophisticated numerical approach would be to consider a minimum area surface at each step of restructuring, its area decreasing gradually during the sintering process. A Monte Carlo modelization of such process is under progress. Moreover, we are presently considering the off-lattice numerical approach as a basis to simulate the gas transport properties of partially densified aerogels in order to interpret some new experiments on the permeability of gas [15].

We would like to acknowledge discussions with Marie Foret, Jacques Pelous, René Vacher and Peter Pfeifer. One of us (A. H.) would like to acknowledge support from CONICIT (Venezuela).

REFERENCES

- [1] W. D. Kingery and M. Berg, J. Appl. Phys., **26**, 1205, 1955.
- [2] J. Frenkel, J. Phys. (Moscow), **9**, 385, 1945.
- [3] J. K. Mackenzie and R. Shuttleworth, Proc. Phys. Soc. London, **62**, 833, 1949.
- [4] G. W. Scherer, J. Amer. Ceram. Soc, **60**, 236, 1977; *ibid.*, **60**, 243, 1977.
- [5] G. W. Scherer, J. Amer. Ceram. Soc., **74**, 1523, 1991.
- [6] R. Sempéré, D. Bourret, T. Woignier, J. Phalippou and R. Jullien, Phys. Rev. Lett., **71**, 3307, 1993.
- [7] A. Hasmy, É. Anglaret, M. Foret, J. Pelous and R. Jullien, Phys. Rev. B, **50**, 1305, 1994; see also A. Hasmy, É. Anglaret, M. Foret, J. Pelous, R. Vacher and R. Jullien, in this issue of J. of Non Cryst. Sol.
- [8] B. B. Mandelbrot, “The Fractal Geometry of Nature”, Freeman, New-York, 1982.
- [9] P. Meakin, Phys. Rev. Lett., **51**, 1119, 1983.
- [10] M. Kolb, R. Botet and R. Jullien, Phys. Rev. Lett., **51**, 1123, 1983.
- [11] A. Hasmy, M. Foret, J. Pelous and R. Jullien, Phys. Rev. B, **48**, 9345, 1993.
- [12] S. Ma, “Modern Theory of Critical Phenomena”, Benjamin, New-York, 1976.
- [13] R. Jullien and R. Botet, Aggregation and fractal aggregates, World Scientific, Singapore, 1987.
- [14] T. Woignier, habilitation report, University of Montpellier II, unpublished.
- [15] A. Hasmy, I. Beurroies, D. Bourret and R. Jullien, preprint.

TABLES

c_0	a_f	ξ_0	ξ'_0
0.01	6.2	23	28.8
0.02	4.6	13.5	16.9
0.05	3.2	6.1	8.7
0.077	2.5	4.0	5.9
0.1	2.3	3.0	5.0

TABLE I. For each concentration c_0 considered in the off-lattice simulations, we have reported the value of a_f , the corresponding value of ξ_0 and the location ξ'_0 of the minimum of the pair correlation function $g(r)$.

FIGURES

FIG. 1. Two dimensional sketch of an individual aggregate at two different stages of sintering.

FIG. 2. Section of the box for the original configuration and at two stages of sintering. (a) and (b) correspond to the on-lattice (with $L = 32$) and off-lattice (with $L = 40$) method respectively.

FIG. 3. Log-log plot of a/a_0 and ξ/a_0 versus $c = \rho/\rho_S$ for $L = 64$ and different initial concentrations c_0 . Cases (a) and (b) correspond to the on-lattice and off-lattice method respectively. In case (a) open circles, black squares, open diamonds and black triangles correspond to $c_0 = 0.01, 0.02, 0.05$ and 0.1 , respectively. The solid lines are the results for ξ/a_0 . The dashed curve shown in (a) corresponds to the off-lattice results with $c_0 = 0.01$.

FIG. 4. Log-log plot of Σ/Σ_0 versus $c = \rho/\rho_S$ for $L = 64$ and different initial concentrations c_0 . Cases (a) and (b) correspond to the on-lattice and off-lattice method respectively. In case (a) open circles, black squares, open diamonds and black triangles correspond to $c_0 = 0.01, 0.02, 0.05$ and 0.1 , respectively. The dashed curve shown in (a) corresponds to the off-lattice results with $c_0 = 0.01$.

FIG. 5. Low angle neutron scattering intensity curves $I(q)$ for a series of neutral PDA with increasing density.

FIG. 6. Experimental dependences of a/a_0 (black symbols) and ξ/a_0 (open symbols) as a function of $c = \rho/\rho_S$ (log-log plots) for a basic sample (case a) and for two neutral samples (case b). In case (a) the full line is the theoretical curve obtained with the off-lattice model with $c_0 = 0.04$ and the open circles are the results obtained with the on-lattice model with $c_0 = 0.08$.

fig 3a

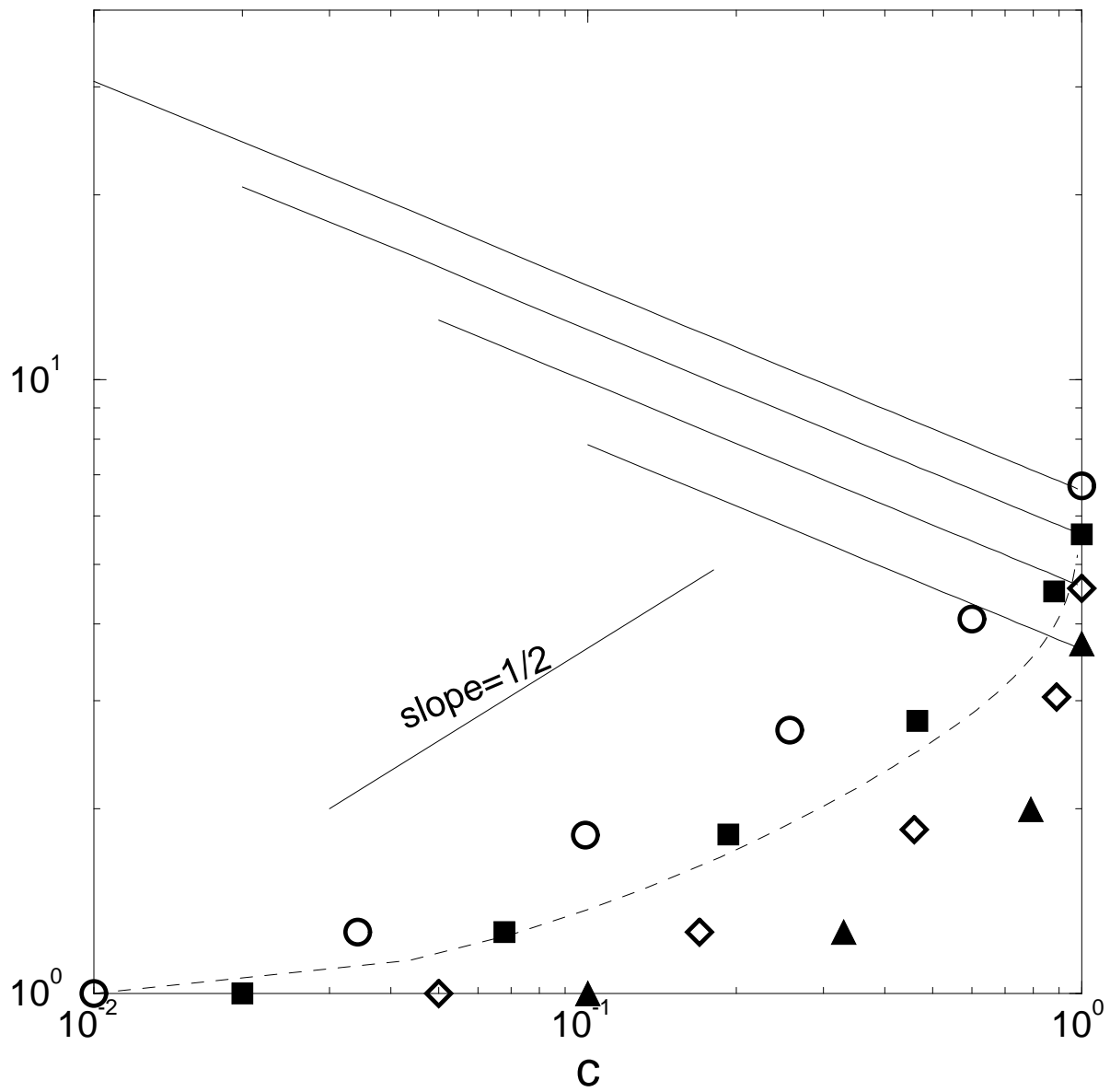


fig 3b

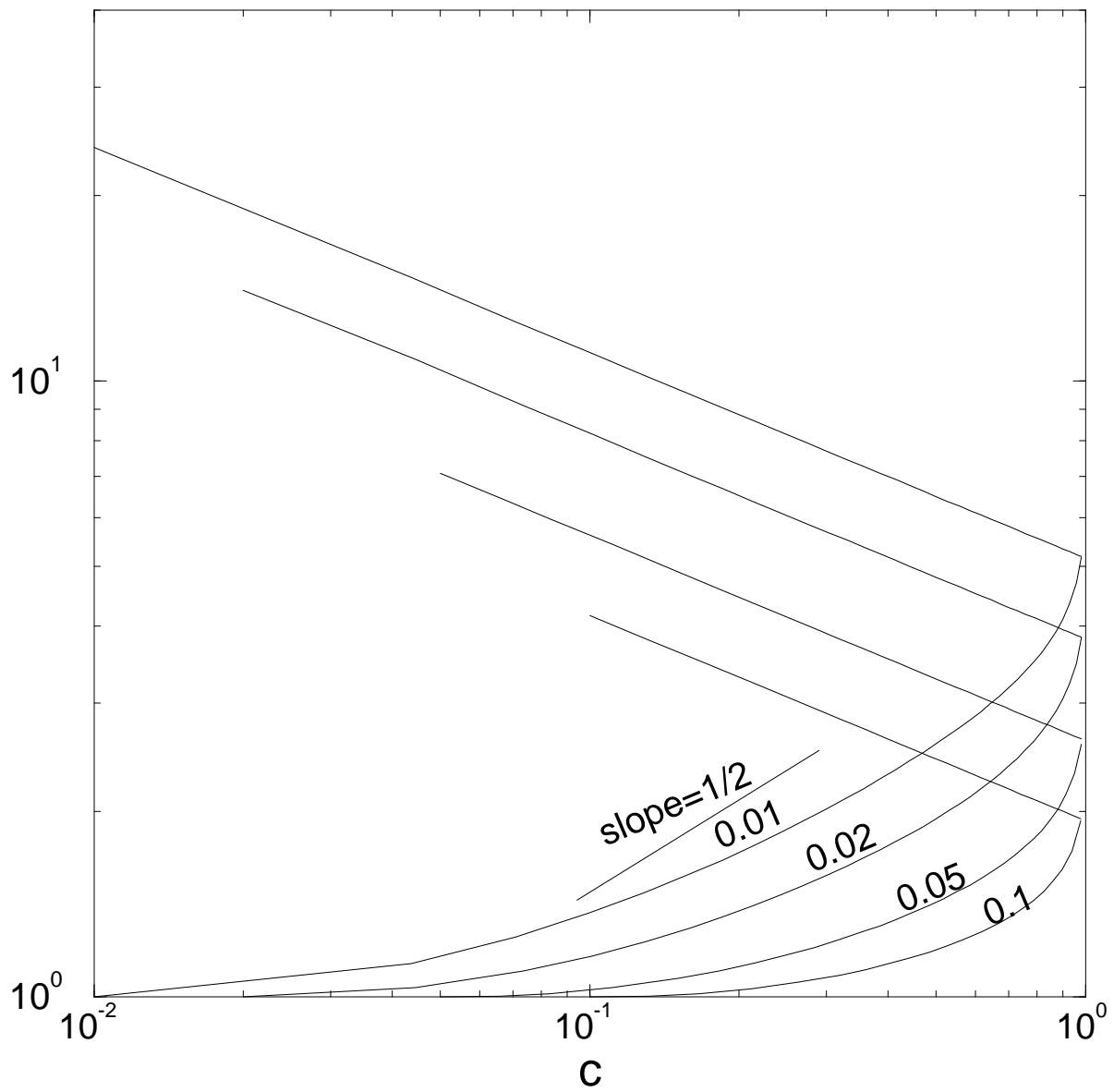


fig 4a

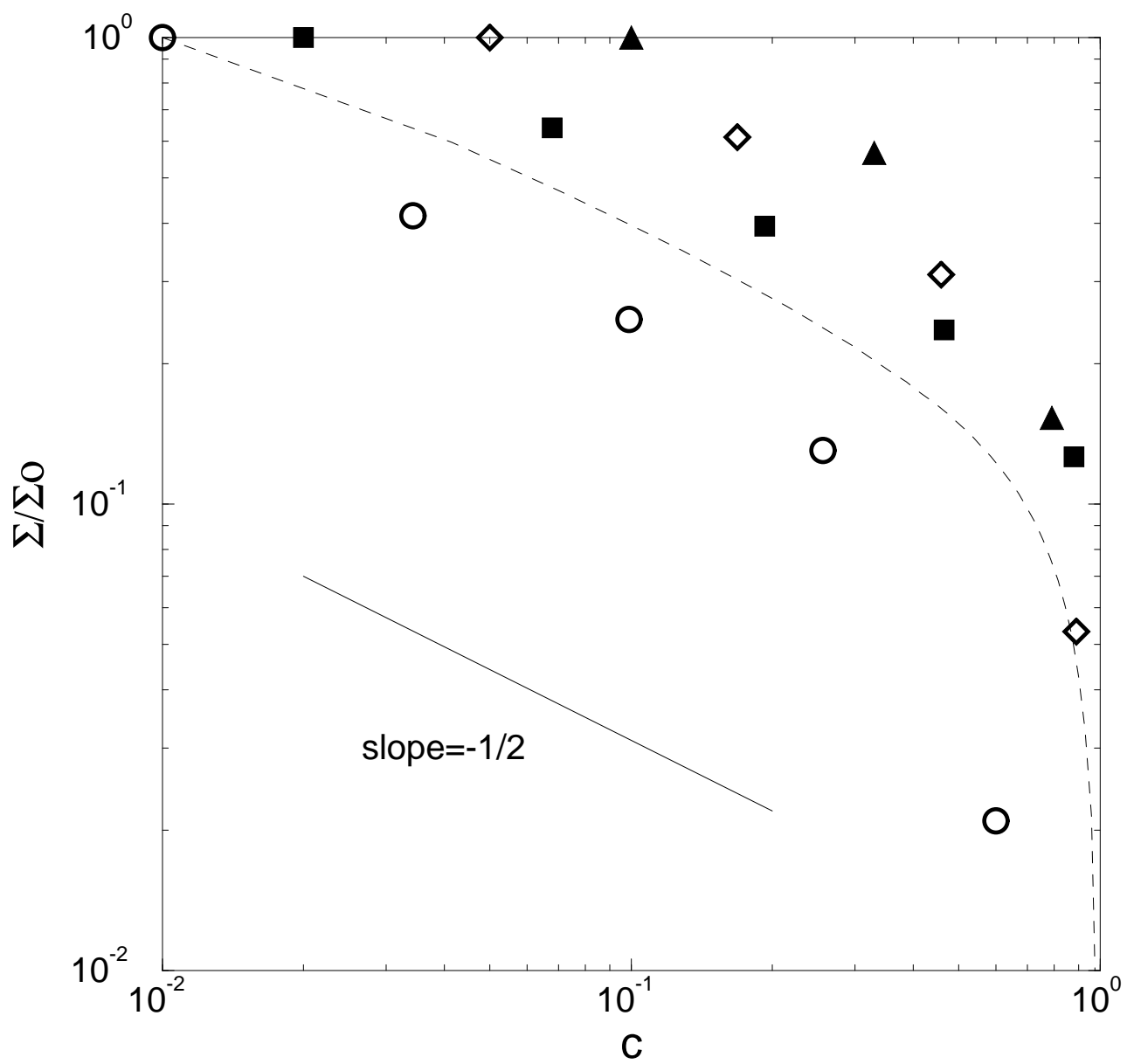


fig 6a

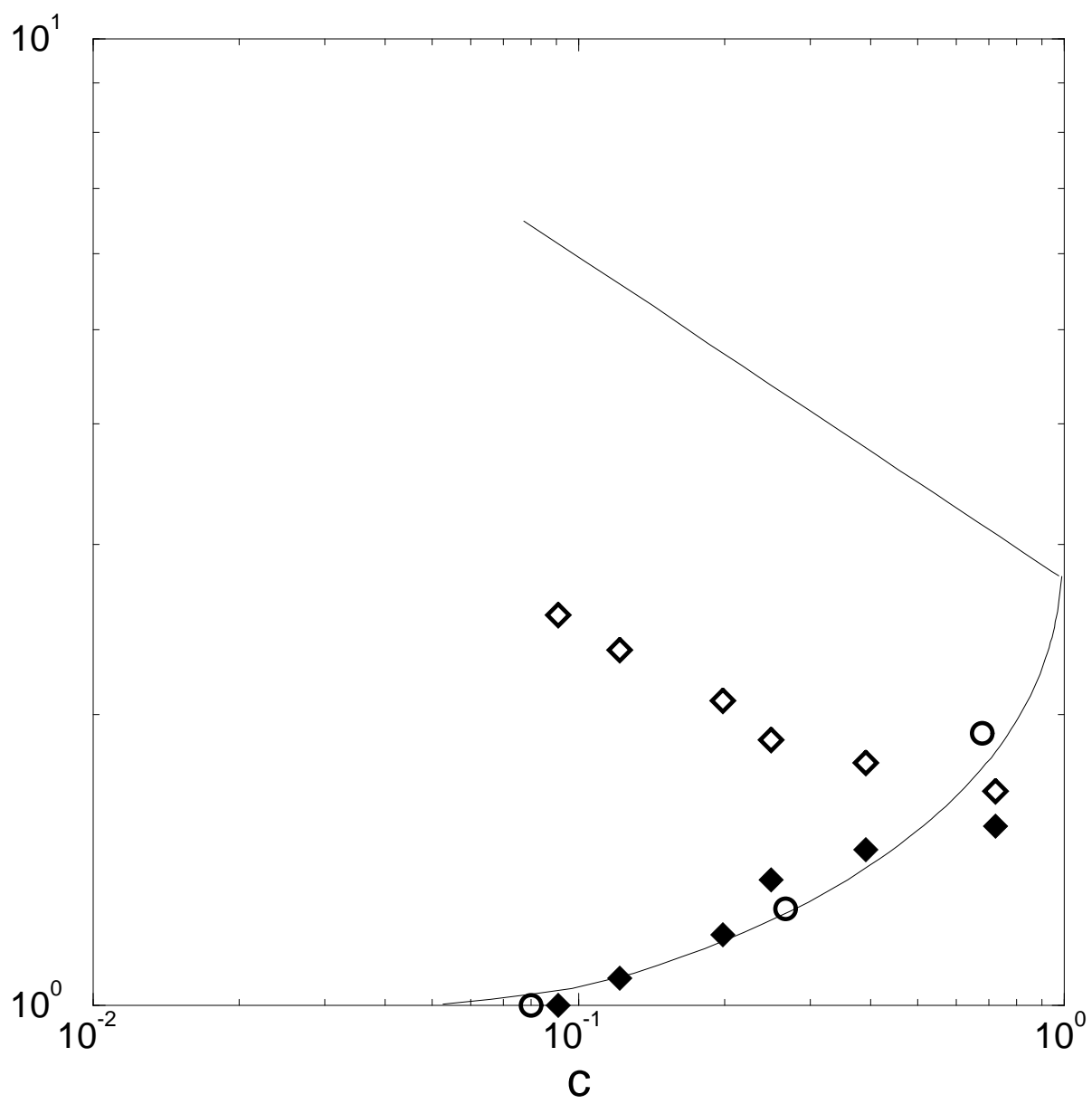


fig 6b

